

Satellite Fault Detection and Isolation Scheme with Modified Adaptive Fading EKF

Jun Kyu Lim* and Chan Gook Park[†]

Abstract – This paper presents a modified adaptive fading EKF (AFEKF) for sensor fault detection and isolation in the satellite. Also, the fault detection and isolation (FDI) scheme is developed in three phases. In the first phase, the AFEKF is modified to increase sensor fault detection performance. The sensor fault detection and sensor selection method are proposed. In the second phase, the IMM filter with scalar penalty is designed to detect wherever actuator faults occur. In the third phase of the FDI scheme, the sub-IMM filter is designed to identify the fault type which is either the total or partial fault. An important feature of the proposed FDI scheme can decrease the number of filters for detecting sensor fault. Also, the proposed scheme can classify fault detection and isolation as well as fault type identification.

Keywords: Satellite, Fault detection, Fault identification, AFEKF, IMM, Total failure, Partial fault

1. Introduction

The spacecraft's attitude control system (ACS) faults caused by malfunctions in its sensors, actuators and components result from unexpected interferences or gradual aging of system components. These faults could result in higher energy consumption, loss of the vehicle control, and in case of total failures, catastrophic loss of the satellite [1-5].

The increasing complexity of space vehicles has necessitated calls for increasingly more autonomy in the spacecraft control system. If the satellite has malfunctions or anomalies, the satellite's operation mode is changed to safe-mode. General methods for detecting and correcting abnormal phenomenon in the satellite are operated on the ground station. Traditionally, health monitoring and trend analysis of satellite telemetry data have been a time-consuming, repetitive, and labor-intensive activity. Therefore, it is slow, accumulated error and interrupted mission. It should be treated automatically in the satellite [1, 3, 6, and 7].

The most common approach to provide a system with fault detection and isolation (FDI) functionality is to use hardware redundancy. The basic concept of hardware redundancy is to compare duplicative signals generated by various hardware such as measurements of the same signal given by two or three sensors. The main drawback with the hardware redundancy approach is to increase complexity and costs resulting from the additional weight

and volume of the redundant elements [8]. On the other hand, analytical redundancy uses a mathematical model of the system together with some estimation techniques for FDI. As the analytical redundancy approach generally does not require additional hardware, it is usually a more cost effective approach compared to the hardware redundancy approach [1, 3, 9-11].

Model-based fault detection has been employed in the Cassini satellite. A set of three model-based leakage detection monitors has been designed and implemented in the flight software to protect Cassini against the occurrence of unlikely event [12].

In the multiple model adaptive estimation (MMAE) approach, a bank of Kalman filters runs in parallel independently. Such an approach is effective in handling problems with unknown but constant structures or parameters [7]. However, the problem of fault diagnosis and reconfigurable control may not fit well into such a framework because, in general, the system structure or parameter changes as a component or a subsystem fails. To overcome this weakness and to make multi model algorithms better suited for the fault detection and diagnosis, the interacting multiple model (IMM) approach has been proposed in [6]. In the IMM approach, the occurrence or recovery of a failure in a dynamic system has been explicitly modeled as a finite-state Markov chain with known transition probabilities. The IMM algorithm considers the structural changes of the system discussed explicitly by Gaussian approximations and a hypothesis merging technique known as "mixing" [13].

The performance of the IMM algorithm for FDI has been showed in [13]. An FDI technique using a fuzzy-tuned IMM filter for aircraft flight control system has been showed in [14]. Fuzzy logic is used to tune a transition probability among multiple models. The development and

[†] Corresponding Author: Dept. of Mechanical and Aerospace Engineering & Automation and Systems Research Institute, Seoul National University, Korea. (chanpark@snu.ac.kr)

* Dept. of Mechanical and Aerospace Engineering & Automation and Systems Research Institute, Seoul National University, LIG Nex1, Korea. (nesljk@snu.ac.kr)

Received: August 23, 2013; Accepted: January 13, 2014

testing of FDI method is considered in [15]. It was based on IMM filters for both partial (soft) and total (hard) reaction wheels faults in a spacecraft. The FDI method for LEO satellite attitude determination and control system by checking the statistical characteristics of EKF innovation sequence is proposed [16]. It is based on statistics for the mathematical expectation of the spectral norm of the normalized innovation matrix of the EKF. The FDI method is proposed in the navigation and control system of deep space satellites. In addition, the method uses the Shirayev sequential probability ratio test to estimate the probability of the fault signal given the residuals generated from either parity relationships, fault detection filters or GLR test [17, 18]. Patton and Uppal [8, 19] presented a robust approach to FDI residual generator that is described to realize a diagnostic scheme for the satellite system, focused on a thruster modulation problem and presented a practical solution to the problem of robust FDI for a satellite system Mars Express (MEX).

However, these approaches are inefficient in detecting fault when the fault type is different. Also, if the IMM filter is used for sensor and actuator fault FDI, too many fault models will be needed. Thus, we proposed a cascade filter structure for sensor/actuator FDI method and multi-hypothesis filter for fault tolerant attitude estimation of LEO satellite in [20, 21 and 29]. The decentralized Kalman filter (DKF) and IMM filter were used for sensor and actuator FDI in [20]. In this paper, the modified adaptive fading EKF (AFEKF) is proposed for sensor FDI. A novel FDI scheme using the modified AFEKF for sensor FDI and two-step IMM filter for actuator FDI is proposed. With this proposed method, the AFEKF can reduce the number of filters compared with DKF and keep the FDI performance. Fig. 1 shows the cascade filter structure using the DKF and IMM filter. When the DKF is utilized for detection and diagnosis of sensor fault, the DKF has to use at least three filters. The DKF includes two local filters, which are two full states EKF, and sensitivity calculation and one master filter. The first local filter obtains an estimation

value of a satellite attitude model using the measurement of the first sensor module and the second local filter obtains an estimation value using the second sensor module measurement. The sensitivity factors of the first and second local filters are calculated. Then, we compare two sensitivity factors to detect sensor fault. If one of the sensitivity factors is larger than a threshold value, we decide that the sensor module has a fault. The master filter only uses other local filter data and not data from the fault sensor module. However, the modified AFEKF requires only one filter for sensor FDI. The proposed scheme can detect and identify the fault on satellite actuator and sensor. Moreover, the AFEKF can eliminate abnormal instantaneous sensor measurements.

In section 2, a satellite dynamic model is introduced. This paper develops the general nonlinear model of a satellite with thrusters and four reaction wheels. Due to the nonlinearity of the problem, the EKF was used in the AFEKF and IMM filter. In section 3, the proposed scheme is presented. The FDI procedure is developed in three phases. In section 4, the modified AFEKF is described. The AFEKF is modified to increase sensor fault detection performance. The fault detection and sensor selection method are proposed. In section 5, the simulation results have demonstrated the advantages of proposed FDI scheme. Finally, section 6 provides conclusion.

2. Satellite Dynamic Model

2.1 Nonlinear satellite attitude model

The satellite attitude model is discussed by defining the LVLH (Local Vertical Local Horizontal) coordinate. The y-axis of LVLH coordinate is in opposite direction of orbit angular momentum vector of satellite and the z-axis is parallel to the vector from satellite to the mass center of the Earth. The x-axis is decided by the other two axes. The origin of the body-fixed coordinate (BFC) system is fixed

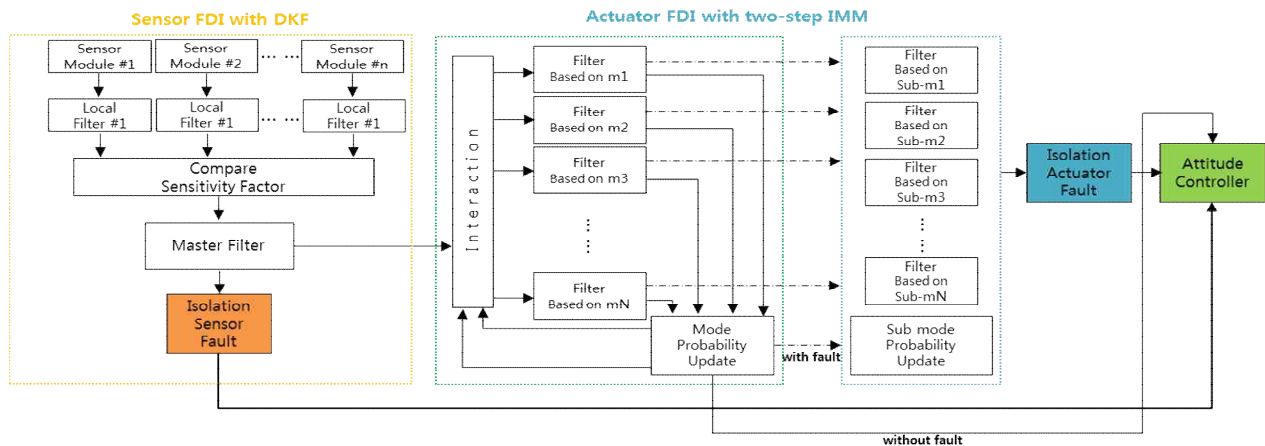


Fig.1. The FDI scheme with DKF and IMM filter

at the satellite mass center and rotates with the satellite at angular rate. Consider the nonlinear satellite attitude dynamics model with four reaction wheels and sixteen thrusters. The model is constructed like Eqs. (1-3) [22-25].

$$\mathbf{I}_g \dot{\underline{\omega}} = -\underline{\omega} \times (\mathbf{I}_t \underline{\omega} + \mathbf{L}^T \mathbf{I}_w \underline{\Omega}) - \mathbf{L}^T \underline{\tau}_{wheel} + \underline{\tau}_{thruster} + \underline{\tau}_{gravity} + \underline{\tau}_{aero} + \underline{\tau}_{magnetic} + \underline{\tau}_{srp} \quad (1)$$

$$\dot{h}_w = \underline{\tau}_w \quad (2)$$

$$\dot{h}_w = \mathbf{I}_w \underline{\Omega} + \mathbf{I}_w \mathbf{L} \underline{\omega} \quad (3)$$

where,

- \mathbf{I}_t : Total moment of inertia for the satellite body (3 × 3),
- \mathbf{I}_w : Moment of inertia matrix for the wheels (4 × 4),
- $\mathbf{I}_g = \mathbf{I}_t - \mathbf{L}^T \mathbf{I}_w$: Total moment of inertia minus the moment of inertia of the wheels (3 × 3),
- \mathbf{L} : Wheel orientation matrix (4 × 3),
- $\underline{\omega}$: Satellite angular velocity vector in Body fixed coordinate (BFC),
- $\underline{\Omega}$: Wheel speed vector,
- $\underline{\tau}_{wheel}$: Absolute torque due to the reaction wheels,
- $\underline{\tau}_{thruster}$: Torque due to the thrusters,
- $\underline{\tau}_{gravity}$: Torque due to the Earth's gravity gradient,
- $\underline{\tau}_{aero}$: Aerodynamic torque due to the atmospheric drag,
- $\underline{\tau}_{magnetic}$: Torque due to the thrusters,
- $\underline{\tau}_{srp}$: Torque due to the thrusters,
- h_w : Angular momentum of the wheel cluster,

Fig. 2 shows the configuration of reaction wheels. There are only three reaction wheels needed to control three dimensional spacecraft attitude. One reaction wheel is included as a hardware redundancy for the fault situation. The cone shape is known for the most efficient configuration with four reaction wheels [24-25]. The orientation matrix is given by

$$\mathbf{L} = \begin{pmatrix} \sin \beta \cos \sigma & \sin \beta \sin \sigma & \cos \beta \\ -\sin \beta \cos \sigma & \sin \beta \sin \sigma & \cos \beta \\ -\sin \beta \cos \sigma & -\sin \beta \sin \sigma & \cos \beta \\ \sin \beta \cos \sigma & -\sin \beta \sin \sigma & \cos \beta \end{pmatrix} \quad (4)$$

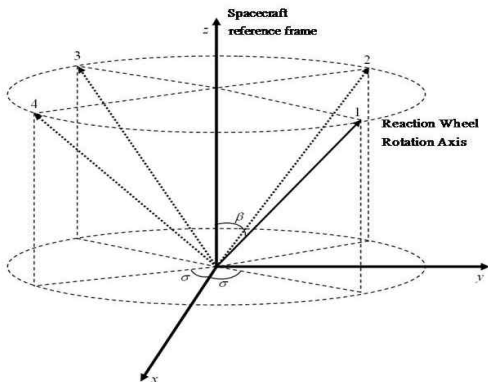


Fig. 2. Reaction wheel configuration

From the Eqs. (1-3), we obtain the wheel dynamic equation. The time derivative of Eq. (3) is added to Eq. (2) and solved for $\underline{\Omega}$. Then following equation can be obtained.

$$\underline{\dot{\Omega}} = \mathbf{I}_w^{-1} \underline{\tau}_{wheel} - \mathbf{L} \underline{\dot{\omega}} \quad (5)$$

Substitute Eq. (1) into Eq. (5) to obtain,

$$\underline{\dot{\Omega}} = \mathbf{I}_w^{-1} \underline{\tau}_{wheel} - \mathbf{L} [-\mathbf{I}_g^{-1} \underline{\omega} \times (\mathbf{I}_t \underline{\omega} + \mathbf{L}^T \mathbf{I}_w \underline{\Omega}) + \mathbf{I}_g^{-1} \left(-\mathbf{L}^T \underline{\tau}_{wheel} + \underline{\tau}_{thruster} + \underline{\tau}_{gravity} + \underline{\tau}_{aero} + \underline{\tau}_{magnetic} + \underline{\tau}_{srp} \right)] \quad (6)$$

In this paper, we assume the deep space satellite. Thus, we can only consider Euler equation or the gyroscopic torque of reaction wheels and the absolute torque of reaction wheels and thrusters. We consider the dynamic model as Eq. (7).

$$\mathbf{I}_g \underline{\dot{\omega}} = -\underline{\omega} \times (\mathbf{I}_t \underline{\omega} + \mathbf{L}^T \mathbf{I}_w \underline{\Omega}) - \mathbf{L}^T \underline{\tau}_{wheel} + \underline{\tau}_{thruster} \quad (7)$$

From Eqs. (7) and (5), we can obtain Eq. (8).

$$\underline{\dot{\Omega}} = \mathbf{I}_w^{-1} \underline{\tau}_{wheel} + \mathbf{L} [\mathbf{I}_g^{-1} \underline{\omega} \times (\mathbf{I}_t \underline{\omega} + \mathbf{L}^T \mathbf{I}_w \underline{\Omega}) + \mathbf{I}_g^{-1} (\mathbf{L}^T \underline{\tau}_{wheel} + \underline{\tau}_{thruster})] \quad (8)$$

where $\underline{\omega} = [\omega_x, \omega_y, \omega_z]^T$ is angular velocity vector in BFC. Attitude control requires coordinate transformation from LVLH to BFC. The satellite body axis has to be aligned with LVLH axis. The system of differential equation describing the vehicle attitude is defined by

$$\begin{bmatrix} \dot{\phi} \\ \dot{\theta} \\ \dot{\psi} \end{bmatrix} = \frac{1}{\cos \psi} \begin{bmatrix} \cos \psi & -\cos \phi \sin \psi & \sin \phi \sin \psi \\ 0 & \cos \phi & -\sin \phi \\ 0 & \sin \phi \cos \psi & \cos \phi \cos \psi \end{bmatrix} \begin{bmatrix} \omega_x \\ \omega_y \\ \omega_z \end{bmatrix} \quad (9)$$

Fig. 3 shows the general arrangement of sixteen thrusters. Two thrusters always actuate together to control attitude of the satellite without changing trajectory such as using #2 and #10 at the same time. If the satellite tries to generate the linear acceleration for trajectory control, other two actuators are activated such as #4 and #10. That means two

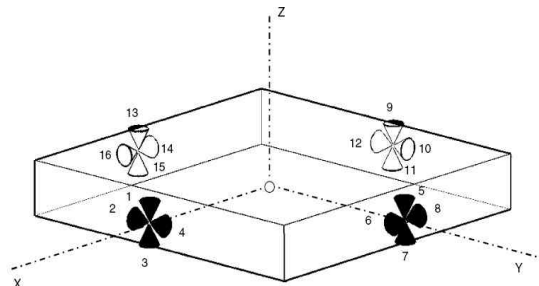


Fig. 3. Thruster configuration

thrusters always work simultaneously to control attitude or linear accelerate. In this paper, we assume that sixteen thrusters are mounted on satellite [17].

3. Fault Detection and Identification Scheme

In this section, the novel FDI scheme of the ACS of a satellite is proposed. This proposed scheme has three main stages. The first stage is the sensor FDI with the modified AFEKF. We modified the AFEKF to increase FDI performance by n square penalty method. The sensor fault detection and selection methods are proposed. The modified AFEKF will be described in section 4. The second stage is the actuator fault detection with the IMM filter. The third stage is the sub-IMM filter for classification fault type. First of all, the system chooses which sensor module will be used through the sensor selection module. The sensor FDI is performed with the AFEKF. The proposed AFEKF can be eliminated abnormal measurement. Thus, the accurate estimated states, which mean the AFEKF gives estimated state like no fault situation, are transferred to the IMM filter for actuator FDI. If sensor has fault, the sensor selection module selects next sensor using the fault information, which is performed in the isolation sensor fault block. The second stage is actuator FDI. First of all, the IMM filter performs twenty actuators fault detection. If the actuators have no fault, the sub-IMM filter does not operate in the third stage. It is activated only the actuator fault situation. The sub-IMM filter has same filter structure compared with the IMM filter of second stage. The sub-IMM filter has four fault model, which are total failure and three partial fault models. The proposed scheme is presented in Fig. 4.

3.1 Extended kalman filter

The Kalman filtering problem considered up to this

point in the discussion has addressed the estimation of a state vector in a linear model of a dynamical system. However, if the model is nonlinear, we may extend the use of Kalman filtering through a linearization procedure. The resulting filter is referred to as the extended Kalman filter (EKF) [26]. The EKF linearizes the nonlinear dynamics by calculating the Jacobian at each time step. The state vector x consists of satellite attitude vector, angular velocity vector and wheel speed vector. Input vector given in Eq. (11) consists of four reaction wheels and three axis thrusters [20].

$$\dot{x} = \left(\frac{\partial f}{\partial x'} \right) x + \left(\frac{\partial f}{\partial u'} \right) u \quad (10)$$

$$x = [\phi, \theta, \psi, \omega_x, \omega_y, \omega_z, \Omega_1, \Omega_2, \Omega_3, \Omega_4]^T$$

$$u = [\tau_{w1} \ \tau_{w2} \ \tau_{w3} \ \tau_{w4} \ \tau_{x-thrust} \ \tau_{y-thrust} \ \tau_{z-thrust}]^T \quad (11)$$

To make it simple, moments of the inertial matrix for the wheels and satellite body are defined by

$$I_w = \begin{bmatrix} I_{w1} & 0 & 0 & 0 \\ 0 & I_{w2} & 0 & 0 \\ 0 & 0 & I_{w3} & 0 \\ 0 & 0 & 0 & I_{w4} \end{bmatrix}, I_t = \begin{bmatrix} I_x & 0 & 0 \\ 0 & I_y & 0 \\ 0 & 0 & I_z \end{bmatrix} \quad (12)$$

The partial derivative matrix for this system is written by

$$\frac{d}{dt} x = Ax + Bu$$

$$A = \begin{bmatrix} A_{11} & A_{12} & 0_{3 \times 4} \\ 0_{3 \times 3} & A_{22} & A_{23} \\ 0_{4 \times 3} & A_{32} & A_{33} \end{bmatrix}, B = \begin{bmatrix} 0_{3 \times 4} & 0_{3 \times 3} \\ -I_g^{-1} L^T & I_g^{-1} \\ I_w^{-1} + L I_g^{-1} L^T & -L I_g^{-1} \end{bmatrix} \quad (13)$$

The measurement equation is given by

$$z = Hx + v \quad (14)$$

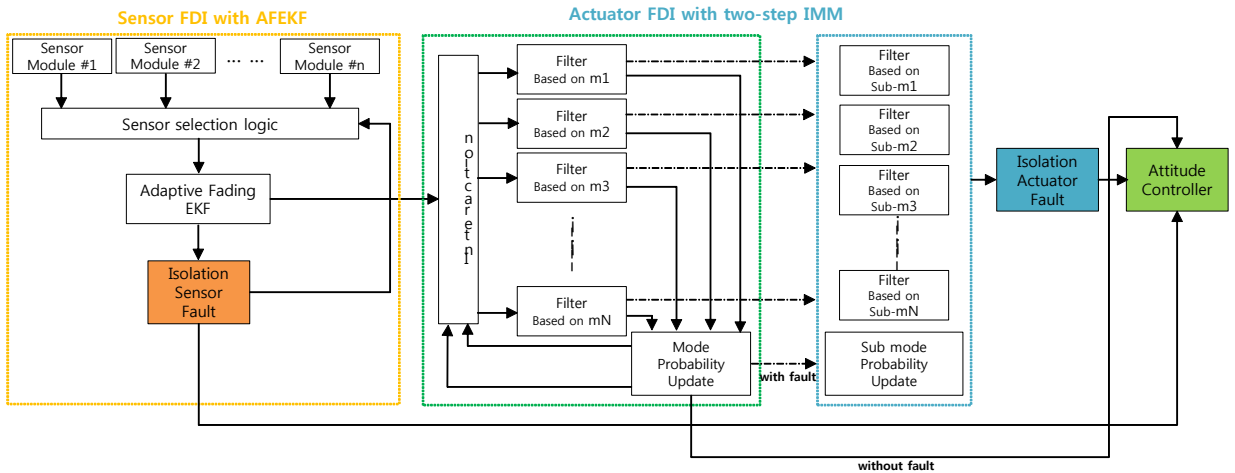


Fig. 4. The FDI scheme of the satellite attitude control system

where H is defined by identity matrix 10×10 and variable v is the measurement noise vector considered to be white Gaussian. The measurement vector z consists of vehicle attitude vector, angular velocity vector and wheel speed vector.

3.2 Two-step IMM filter

The interacting multiple model (IMM) filter is one of the most cost-effective adaptive estimation techniques for systems involving structural as well as parametric changes [6, 7]. In the paper, the IMM is used for actuators FDI which are thrusters and reaction wheels. The IMM is a bank of Kalman filter. Several Kalman filters perform parallel in the same time.

The conventional IMM filter can detect a fault, but the filter can not classify fault types. For example, if the first reaction wheel has a total fault, which means the reaction wheel is completely stopped, the conventional IMM filter can detect a fault well. However, if the first reaction wheel has a partial fault, the IMM filter can detect the fault, but it can not classify what kind of fault is occurred. If the IMM filter can detect both total and partial fault, the IMM filter has to have both fault model for each actuators. We consider sixteen thrusters and four reaction wheels. In that case, the conventional IMM filter has to have over fifty fault models.

However, the two-step IMM filter requires only eleven total fault models and four partial fault models, since the two-step IMM filter detects actuator fault first. If the specific actuator has a fault, the sub-IMM performs for the fault type classification using four partial fault models. The reason for the eleven fault models are needed, two thrusters always work simultaneously to control attitude. Thus, two models for the each x-axis thruster (+, -), y-axis thruster (+, -), z-axis thruster faults and four reaction wheel faults and normal model.

To detect an actuator fault, the IMM filter uses residuals and residual covariance of each filter as following equations

$$v_{jk} = z_k - H_{jk}(\hat{x}_{jk}^-), \quad j = 1, 2, \dots, N \quad (15)$$

$$S_{jk} = H_{jk}P_{jk}^-H_{jk}^T + R_{jk} \quad (16)$$

where j is the model number. For example, if the normal model or no fault model label is 1, this model residual is denoted as v_1 . The most important part is likelihood function computation and mode probability update. This is the main different comparing with the conventional Kalman filter. The fault detection method using the IMM filter determines the fault when the mode probability obtained through the residual between the fault model and the current system is larger than threshold.

A likelihood function for calculating mode probability in the IMM filter is as the following equation:

$$L_{jk} = \frac{1}{\sqrt{|(2\pi)S_{jk}|}} \exp\left[-\frac{1}{2}v_{jk}^T S_{jk}^{-1}v_{jk}\right] \quad (17)$$

If the magnitude of the fault is large enough, a difference between the respective models is large so that the fault can be immediately detected. However, if the magnitude of the fault is small and variation in residual due to the fault is also small, the fault can be detected under the condition that the residuals are accumulated. Therefore, a time delay is occurred. For this reason, in order to reduce a fault detection time which is a disadvantage of the fault detection method using the conventional IMM filter, and simultaneously, to increase detection performance of a relatively small fault, a penalty κ is used to the model probability in this paper [4, 20].

$$L_{jk} = \frac{1}{(2\pi)^{m/2}\sqrt{|S_{jk}|}} \exp\left[-\kappa \cdot \frac{1}{2}v_{jk}^T S_{jk}^{-1}v_{jk}\right] \quad (18)$$

where m is the dimension of the measurement vector. Using this likelihood, the mode probability can be calculated as

$$\mu_{jk} = \frac{\mu_{jk}^- L_{jk}}{\sum_1^N \mu_{jk}^- L_{jk}} \quad (19)$$

The above mode probability provides an indication of the fault. A fault threshold μ_T is probability value. We can determine μ_T from 0 to 1. We consider that μ_T is the probability cross point. The fault detection method using the mode probability may be accomplished through:

$$\mu_{jk} = \max \mu_{jk} \begin{cases} > \mu_T \Rightarrow H_j : \text{fault } j \text{ occurred} \\ < \mu_T \Rightarrow H_1 : \text{no fault} \end{cases} \quad (20)$$

Using this scheme, the two-step IMM filter can detect fault location and fault types having less fault models at the same time.

4. Modified Adaptive Fading EKF

In this paper, the AFEKF is modified for the sensor FDI. We considered only rescaling Kalman gain and added fault detection and sensor selection methods. To increase small fault FDI performance, the n square penalty methods is proposed. The AFEKF is very adequate filtering algorithm for incomplete dynamic equation, which has incomplete process noise covariance, unknown input bias or incomplete model coefficients, and incomplete measurements equation, which is incomplete measurement noise covariance or unknown measurement bias [27]. The

sensor fault is commonly modeled as additive faults in the system [11, 19 and 28]. The fault can be modeled by annihilating the appropriate row(s) of the measurement matrix described as

$$z(k) = [H(k) + L_j]x(k) + v(k) \quad (21)$$

Alternatively, the j -th sensor fault may be modeled by an additional sensor noise term $e_j(k)$.

$$z(k) = H(k)x(k) + v(k) + e_j(k) \quad (22)$$

The Eqs. (10, 14) can be represented as nonlinear discrete-time stochastic system.

$$\begin{aligned} x_{k+1} &= f_k(x_k) + w_k \\ z_k &= h_k(x_k) + v_k \end{aligned} \quad (23)$$

where the w_k and v_k denote sequences of uncorrelated Gaussian random vectors with zero means.

To applied adaptive fading method, the innovation has to be calculated by

$$\eta_k = z_k - h_k(\hat{x}_k^-) \quad (24)$$

The innovation of the filter is easily affected by unknown fault bias. The innovation covariance of the EKF is

$$C_k = E[\eta_k \eta_k^T] = H_k P_k^- H_k^T + R_k \quad (25)$$

where P_k^- and R_k are a predicted error covariance and a measurement covariance of the EKF. The innovation covariance C_k affected by predicted error covariance and measurement covariance. If both parameters are increased, then C_k is also increased. The increased innovation covariance can be estimated as

$$\hat{C}_k = \frac{1}{M-1} \sum_{i=k-M+1}^k \eta_i \eta_i^T \quad (26)$$

where M is a window size. The relation of two innovation covariance is defined as $\hat{C}_k = \alpha_k C_k$. Then scalar variable α_k (forgetting factor) can be estimated by

$$\alpha_k = \max \left\{ 1, \frac{\text{trace}(\hat{C}_k)}{\text{trace}(C_k)} \right\} \quad (27)$$

In the sensor fault case, the estimation error and the innovation covariance may be also increased by the effect of the unknown information. We consider the measurement

equation is not perfectly known since the equation can be affected by fault. This means that an innovation covariance is increased by an increased measurement covariance. The effects of incomplete information in the measurement equation can be compensated by the decrease of the magnitude of Kalman gain. The decrease of the Kalman gain magnitude means to depend less on measurement information when the sensor has faults. Thus, the Kalman gain can be adjusted as following equation.

$$\bar{K}_k = \frac{K_k}{\alpha_k} = \frac{1}{\alpha_k} P_k^- H_k^T [H_k P_k^- H_k^T + R_k]^{-1} \quad (28)$$

If we want to more sensitive response of filter with small fault, the Eq. (28) can be modified

$$\bar{K}_k = \frac{1}{\alpha_k^n} P_k^- H_k^T [H_k P_k^- H_k^T + R_k]^{-1} \quad (29)$$

where n is a design parameter.

Through the above adaptive method, the proposed AFEKF can offer stable estimation result even in the sensor fault situation. If the forgetting factor has a value greater than 1, this means the measurement is affected by sensor fault. Using this characteristic, we can detect the sensor fault.

$$\alpha_k = \max \left\{ 1, \frac{\text{trace}(\hat{C}_k)}{\text{trace}(C_k)} \right\} \quad (30)$$

$\{ > 1 \Rightarrow f_{id} = 1 : \text{fault occurred in the present sensor module} \}$
 $\{ = 1 \Rightarrow f_{id} = 0 : \text{no fault in the present sensor module} \}$

When the sensor has a fault over 0.5 seconds, which means the 50 angular velocity measurements are offered from the gyro in the 100Hz sampling rate, the sensor selection module switch next gyro module. No reason for the using a fault sensor, even though the AFEKF can eliminate fault measurement. The sensor selection module is performed using the following method.

$$Sw_{id} = \text{cont}\{f_{id}\} \left\{ \begin{aligned} &> 50 \Rightarrow Sw_{id} = 1 : \text{select next sensor module} \\ &< 4 \Rightarrow Sw_{id} = 0 : \text{keep the present sensor module} \\ &\quad \quad \quad \& \text{ no fault alarm} \\ &< 50 \& > 4 \Rightarrow Sw_{id} = 2 : \text{keep the present sensor module} \\ &\quad \quad \quad \& \text{ fault alarm} \end{aligned} \right\} \quad (31)$$

where the $\text{cont}\{f_{id}\} = 3$ is set for preventing false alarm. Since the sensor can be affected by random instantaneous disturbances. In last, the AFEFK can be represented as

following equations

$$\hat{x}_k^- = f_{k-1}(\hat{x}_{k-1}^+) \quad (32)$$

$$P_k^- = F_{k-1}P_{k-1}^+F_{k-1}^T + Q_{k-1} \quad (33)$$

$$\bar{K}_k = \frac{1}{\alpha_k^n} P_k^- H_k^T [H_k P_k^- H_k^T + R_k]^{-1} \quad (34)$$

$$\hat{x}_k^+ = \hat{x}_k^- + \bar{K}_k [z_k - h_k(\hat{x}_k^-)] \quad (35)$$

$$P_k^+ = (I - \bar{K}_k H_k) P_k^- \quad (36)$$

5. Simulation Results

In this section, the proposed FDI scheme is verified by computer simulation. For the satellite attitude estimation, we considered two gyroscope modules for sensor FDI and sixteen thrusters and four reaction wheels for the actuator FDI.

5.1 Scenario 1: (Double Sensor faults)

Sensor fault occurred in x-gyro of module #1 at 2, 3.5, 6 sec and z-gyro at 6 sec. The two types of fault are involved in the simulation. One type is instantaneous fault at 2 and 3.5 sec. Another fault is additive bias type. Fig. 5 shows the angular velocity of the satellite true motion and under the x-gyro and z-gyro measurement with fault.

Fig. 6 shows the sensor fault detection result without switching logic and with switching logic. In the Fig. 6 (a), the proposed filter can detect every abnormal sensor measurements. In the case, the real sensor fault is only after at 6 sec. Two of the abnormal sensor measurements are not actual fault. It is shown as the false alarm case. In the Fig. 6 (b) with switching logic case, the proposed filter detected actual sensor fault. The filter detected only during 6 and 6.5 sec, since the fault has over 0.5 sec. The sensor selection module switches next normal sensor module. This is the sensor fault isolation.

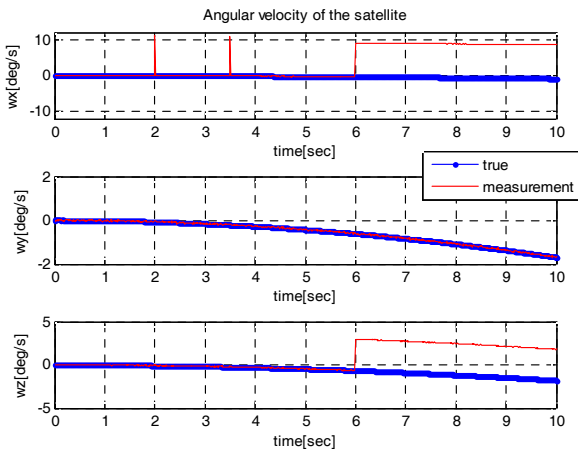
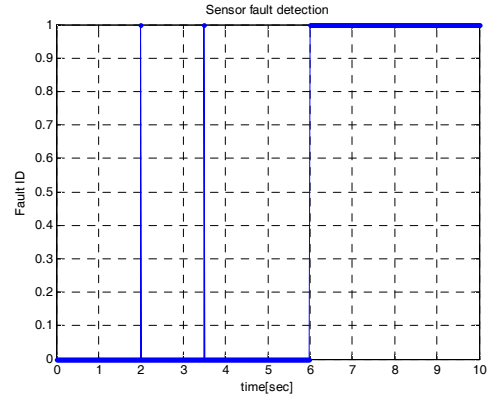
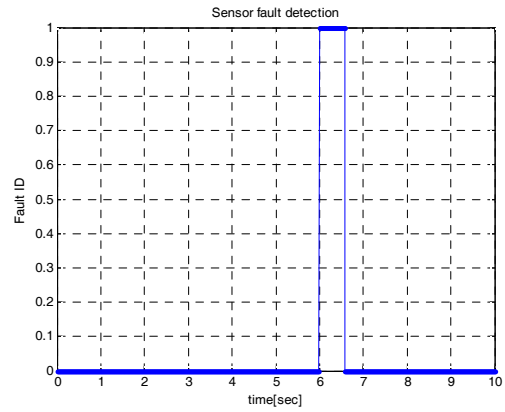


Fig. 5. The angular velocity with sensor fault



(a) Without $S_{W_{id}}$



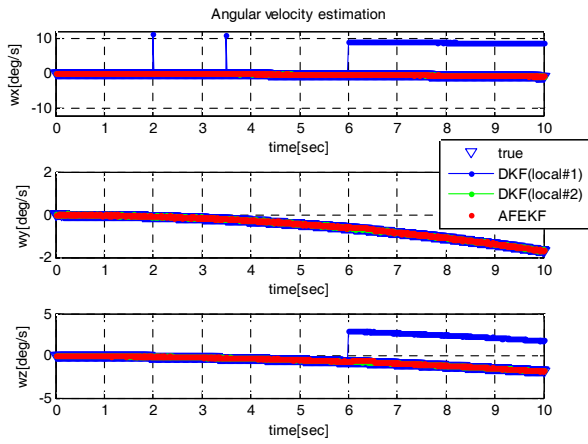
(b) With $S_{W_{id}}$

Fig. 6. Sensor fault detection result

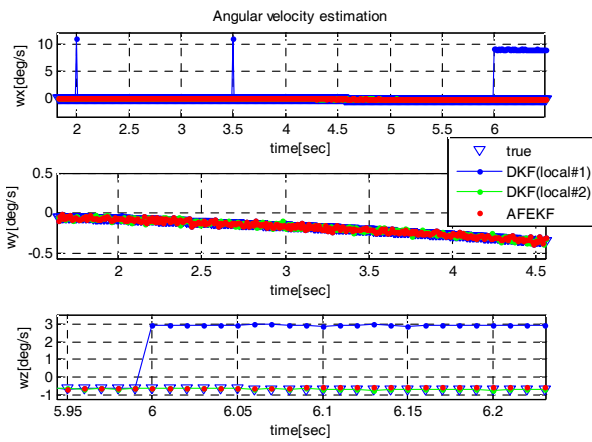
Fig. 7 describes the proposed AFEKF estimation result of angular velocity and the two local filters of the DKF. The AFEKF can reject both instantaneous abnormal and fault measurements. In the sensor fault case, the local filter #1 of DKF has directly influenced by fault. Because the sensor fault was occurred gyro module #1, the local filter #2 of DKF was not influenced by fault. The final DKF estimation result is same as local filter #2 of DKF, since the DKF with FDI is not using fault sensor after sensor FDI. In the proposed scheme Fig. 4, the AFEKF offers the state estimation result to the IMM filter. Thus, accurate state estimation is important. Fig. 7 (b) is the enlarged scale in the abnormal sensor part. We can see the AFEKF is almost perfectly eliminated the abnormal signal. This means that even if the sensor has a fault, the AFEKF can offer accurate state estimation result with double sensor fault situation. Through the Figs. 6 and 7, the proposed AFEKF is verified for sensor FDI and the abnormal measurement rejection performance.

5.2 Scenario 2: (Actuator faults)

In this actuator fault scenario, the reaction wheel #3 fault occurred at 4 sec and the fault magnitude is 75% of normal magnitude. The 75% fault means that the reaction wheel



(a) The angular velocity estimation result



(b) Enlarged scale in sensor abnormal part

Fig. 7. The estimation comparison DKF and AFEKF

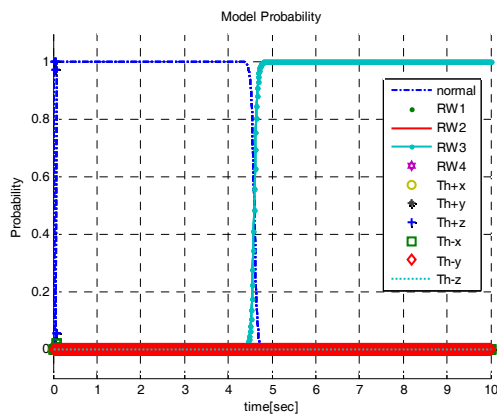


Fig. 8. The model probability with scalar penalty

can give only 25% torque compared with normal torque. The total failure means the reaction wheel is completely stopped.

Fig. 8 shows the fault model probability to detect actuator fault in the first IMM filter with scalar penalty of two-step IMM filter. The probability indicates a normal, which is no fault, before fault occurred. After 4 sec, the

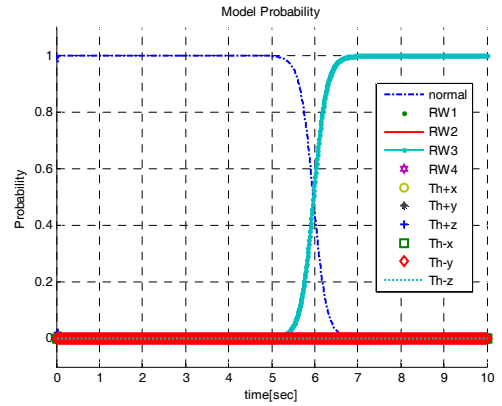


Fig. 9. The model probability without scalar penalty

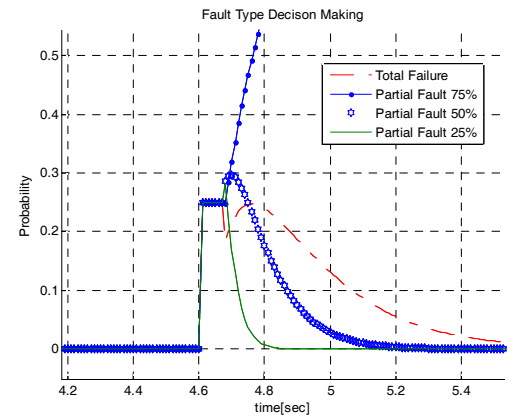
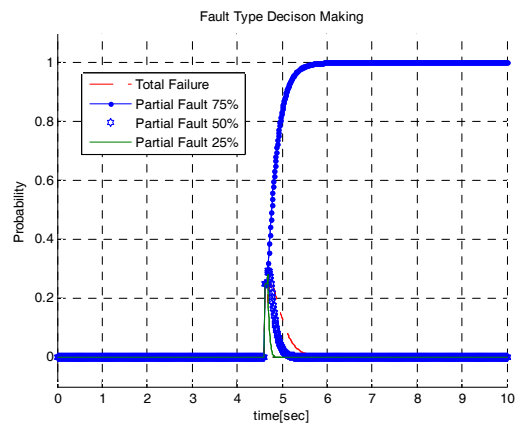


Fig. 10. The actuator fault type classification

model probability of reaction wheel #3 has been changed from 0 to 1. The probability crossing time was 0.6 seconds from 0 to 0.5 after fault occurred.

Fig. 9 shows the same result but only difference is that no scalar penalty was used. In this case, the probability crossing time was 1.9 seconds. It was 1.3 seconds late compared with Fig. 7. Thus, the scalar penalty, which is used for likelihood function calculation, can be reduced fault detection time.

Fig. 10 shows the fault type probability in the sub IMM filter with scalar penalty. The partial fault 75%

model probability is increased before at 5 sec. the bottom figure of Fig. 10 is the enlarged scale during detecting fault type.

6. Conclusion

In this paper, a novel FDI scheme for sensor and actuator fault based on the modified AFEKF and two-step IMM filter was presented. The AFEKF was modified in three parts. First, we considered only rescaling Kalman gain. Second, to increase sensor FDI performance, we suggested a square penalty method for small fault. Third, the sensor FDI and selection method were proposed. Through this proposed filter, we can detect and isolate sensor fault using only one filter. The DKF can be replaced by the proposed AFEKF. Furthermore, the proposed filter can eliminate instantaneous abnormal measurement. The two-step IMM filter was used for actuator FDI with scalar penalty. The IMM filter can detect actuator fault and reduce the fault detection time and classify fault type.

Acknowledgements

This paper is supported by the National Research Foundation of Korea for research number NRF-2013M1A3A3A02042468.

References

- [1] R. Isermann, "Model based fault detection and diagnosis methods," *Proceedings of the American Control Conference*, vol. 3, Washington, 1995.
- [2] R. Isermann. "Process fault detection based on modeling and estimation method-A survey," *Automation*, vol. 20, no. 4, pp.387-404, 1984.
- [3] R. Isermann, *Fault-diagnosis systems-An introduction from fault detection to fault tolerance*, Springer, Germany, 2006.
- [4] P. S. Maybeck and P. D. Hanlon, "Performance enhancement of a multiple model adaptive estimator," *IEEE Trans. on Aerospace and Electronic Systems*, vol. 31, no. 4, pp.1240-1254, 1995.
- [5] K. Narendra and J. Balakrishnan, "Adaptive control using multiple models," *IEEE Trans. on Automatic Control*, vol. 42, no. 2, pp.171-187, 1997.
- [6] Y. Zhang and X. R. Li, "Detection and diagnosis of sensor and actuator failures using IMM estimator," *IEEE Trans. on Aerospace and Electronic Systems.*, vol. 34, no. 4, pp. 1293-1313, Oct. 1998.
- [7] Y. Zhang and X. R. Li, "Detection and diagnosis of sensor and actuator failures using interacting multiple model estimator," *Proceedings of the 36th IEEE Conference on Decision and Control*, pp. 4475-4480, CA, 1997.
- [8] R. J. Patton, F. J. Uppal, S. Simani and B. Polle, "Robust FDI applied to thruster faults of a satellite system," *Control Engineering Practice*, vol. 18, pp. 1093-1109, 2010.
- [9] J. Gertler, "Survey of model-based failure detection and isolation in complex plants," *IEEE Control Systems Magazine*, vol. 8, no. 6, pp. 3-11, 1988.
- [10] M. Tafazoli, "A study of on-orbit spacecraft failures," *Acta Astronautica*, vol. 64, issues 2-3, pp. 195-205, Jan. 2009.
- [11] I. Hwang, S. Kim Y. Kim and C. E. Seah, "A survey of fault detection, isolation, and reconfiguration methods," *IEEE Trans. on Control Systems Technology*, vol. 18, no. 3, pp. 636-653, May. 2010.
- [12] A. Lee, M. Brown, "A model-based thruster leakage monitor for the Cassini spacecraft," *Proceedings of the American Control Conference, IEEE*, pp. 902-904, NJ, 1998.
- [13] Y. Zhang and J. Jiang, "An interacting multiple-model based fault detection, diagnosis and fault tolerant control approach," *Proceedings of the 38th Conference on Decision and Control*, pp. 3593-3598, AZ, 1999.
- [14] S. Kim, J. Choi, and Y. Kim, "Fault detection and diagnosis of aircraft actuators using fuzzy-tuning IMM filter," *IEEE Trans. on Aerospace and Electronic Systems*, vol. 44, no. 3, pp. 940-952, 2008.
- [15] N. Tudoroiu and K. Khorasani, "Satellite fault diagnosis using a bank of interacting kalman filters," *IEEE Trans. on Aerospace and Electronic Systems*, vol. 43, no. 4, pp. 1334-1350, Oct. 2007.
- [16] A. Okatan, Ch. Hajiyev and U. Hajiyeva, "Kalman filter innovation sequence based fault detection in LEO satellite attitude determination and control system," *Recent Advances in Space Technologies, RAST 07. 3rd International Conference*, pp. 411-416, June 14-16. 2007.
- [17] W. R. Williamson, J. L. Speyer, Vu T. Dang and James Sharp, "Fault detection and isolation for deep space satellites," *Journal of Guidance, Control, and Dynamics*, vol. 32, no.5. pp. 1570-1584, Sep. 2009.
- [18] F. N. Pirmoradi and F. Sassani and C.W. de Silva, "Fault detection and diagnosis in a spacecraft attitude determination system," *Acta Astronautica*, vol. 65, issues 5-6, pp. 710-729, Sep. 2009.
- [19] R. J. Patton, "Fault detection and diagnosis in aerospace systems using analytical redundancy," *Computing Control Engineering Journal*, vol. 2, Issue 3, pp. 127-136, May. 1991.
- [20] J. Lee and C. G. Park, "Cascade filter structure for sensor/actuator fault detection and isolation of satellite attitude control system," *International Journal of Control, Automation, and Systems*, vol. 10, no. 3, pp.506-516, 2012.
- [21] J. K. Lim, K. R. Choi and C. G. Park, "Fault tolerant attitude estimation for an LEO satellite using a multi-hypothesis filter," *International Journal of Control, Automation, and Systems*, vol. 10, no. 5, pp.1070-

1076, 2012.

- [22] R. Mehra, S. Seereeram, D. Bayard and F. Hadaegh, "Adaptive Kalman filtering, failure detection and identification for spacecraft attitude estimation," *Proceedings of the 4th IEEE Conference Control Applications*, pp. 176-181, Sept. 1995.
- [23] M. J. Sidi, *Spacecraft Dynamics and Control: A Practical Engineering Approach*, Cambridge University Press, Cambridge, UK, 2000.
- [24] C. H. Won, "Comparative study of various control methods for attitude control of a LEO satellite," *Aerospace Science and Technology*, vol. 3, no. 5, pp. 323-333, 1997.
- [25] C. H. Won, "Satellite structure attitude control with parameter robust risk-sensitive control synthesis," *Proceeding of the 2004 American Control Conference*, pp.3538-3543, Boston, 2004.
- [26] S. Haykin, *Adaptive Filter Theory*, Prentice hall information and system sciences series, Hamilton, Canada, 2002.
- [27] K. H. Kim, J. K. Lee and C. G. Park, "Adaptive two-stage extended Kalman filter for a fault-tolerant INS-GPS loosely coupled system," *IEEE Trans. on Aerospace and Electronic Systems*, vol. 45, no. 1, pp. 125-137, 2009.
- [28] T. E. Menke and P. S. Maybeck, "Multiple model adaptive estimation applied to the VISTA F-16 flight control system with actuator and sensor failures," in *Proceeding. IEEE Nat. Aerosp. Electron. Conference* Dayton, OH, pp. 441-448, May. 1992.
- [29] M. Ilyas, J. K. Lim, J. K. Lee, and C. G. Park, "Federated Unscented Kalman Filter Design for Multiple Satellite Formation Flying in LEO," *International Conference on Control, Automation, and Systems*, Seoul, Korea, pp. 453-458, Oct. 2008.



Chan Gook Park He received the B.S., M.S., and Ph.D. degrees in Control and Instrumentation Engineering from the Seoul National University in 1985, 1987, and 1993 respectively. He worked as a postdoctoral fellow at the Engineering Research Center for Advanced Control and Instrumentation, Seoul National

University in 1993. From 1994 to 2003 he was with the Kwangwoon University, as an Associate Professor. In 2003, he joined the faculty of the School of Mechanical and Aerospace Engineering at the Seoul National University, where he is currently a Professor. In 1998, he worked with Prof. Jason L. Speyer about peak seeking control for formation flight at University of California, Los Angeles (UCLA) as a visiting scholar. His research interests include filtering techniques, inertial navigation systems, GPS/INS integration, and personal navigation systems.



Jun Kyu Lim He received the M.S. degree in School of Mechanical and Aerospace Engineering from Seoul National University in 2008. He is currently working toward a Ph.D degree in School of Mechanical and Aerospace Engineering in Seoul National University and works for LIG Nex1. His

research interests include filtering algorithms and FDI algorithm for spacecraft.